

Optical imaging of BL Lac host galaxies

R. G. Abraham,¹ I. M. McHardy^{1,2} and C. S. Crawford¹

¹*Astrophysics, Department of Physics, University of Oxford, Nuclear Physics Laboratory, Keble Road, Oxford OX1 3RH*

²*Department of Physics, The University, Southampton SO9 5NH*

Accepted 1991 May 31. Received 1991 May 30; in original form 1991 April 15

SUMMARY

We have imaged 23 BL Lacertae objects (BL Lacs) with the William Herschel Telescope in a search for underlying host galaxies. Fourteen of these objects are resolved in our survey. We have determined the morphology of three of these galaxies for the first time, and have confirmed the morphology of an additional three. All the observed underlying hosts are centred on their bright cores, and two of the newly classified hosts are disc systems. These results are in disagreement with the predictions of standard beaming and lensing models for these objects. We have calculated absolute magnitudes for observed hosts with known redshifts and find them to be consistent with the results obtained by previous authors, despite the unexpected morphology exhibited by some of the underlying hosts.

1 INTRODUCTION

BL Lac Objects comprise the most enigmatic class of quasi-stellar objects (QSO). They are characterized by strong flat spectrum radio emission, steep infrared to optical spectra, lack of (or very weak) emission lines, and rapid variability at all wavelengths. The total number of known BL Lacs is small (~ 100), making detailed calculations of their luminosity function difficult (Padovani & Urry 1990, 1991; Maccacaro *et al.* 1989), but it is clear that their redshift distribution is strongly skewed towards lower redshifts ($z \leq 0.2$) relative to the quasar distribution (Wolter & Setti 1982). Very little is known about the nature of BL Lac host galaxies. Imaging studies have generally been hard-pressed to resolve underlying hosts in BL Lacs at all, let alone determine morphology or colours for these galaxies, but classifications have been obtained for around 15 of the nearest BL Lac hosts (Ulrich 1989). With one exception (PKS 1415 + 259; Halpern *et al.* 1986), all BL Lac host galaxies studied prior to our survey were classified as ellipticals, with absolute magnitudes typical of the optical counterparts of Fanaroff-Riley type I (FR I) radio sources (Ulrich 1989).

Simple synchrotron models are unable to explain the properties of BL Lacs because of the ‘Compton Catastrophe’ implied by the apparent large flux and small size of the emitting region in BL Lacs (Hoyle, Burbidge & Sargent 1966; Marscher & Gear 1985). This failure has prompted the emergence of a number of competing models to explain the properties of BL Lacs, the most widely accepted of which was originally put forward by Blandford & Rees (1978). This model postulates the existence of a synchrotron-emitting relativistic jet orientated at a close angle to the observer’s line-of-sight. A natural combination of the ‘relativistic head-

light effect’, Doppler shifting of the continuum, and time dilation accounts for both the large observed flux and rapid variability seen in BL Lacs. Later refinements in the model (Browne 1983) postulate that the parent population of the BL Lacs are the FR I radio galaxies, whose absolute magnitudes are similar to those of known BL Lac hosts, and whose cosmologically non-evolving number counts may (Padovani & Urry 1990, 1991), or may not (Wolter *et al.* 1991), allow a solution to the problem of the strange redshift distribution exhibited by BL Lacs. This model ties in nicely with the all-encompassing ‘unified scheme’ model (Barthel 1989) for active galactic nuclei (AGN), which postulates that the properties of broad line radio galaxies and quasars can be reconciled in a similar fashion.

Another well-known model for BL Lacs was put forward by Ostriker & Vietri (1985), who suggest that at least some BL Lacs are distant Optically Violently Variable (OVV) quasars being gravitationally microlensed by nearby foreground galaxies. OVV quasars differ from BL Lac Objects by exhibiting more prominent lines and by following the conventional quasar redshift distribution. Ostriker & Vietri calculate that the microlensing of a spatially small ($\leq 10^{-3}$ kpc) synchrotron emitting region in an OVV quasar would explain both the dominant continuum in BL Lacs (since the line emitting region is too large to be lensed) and their skewed redshift distribution. The probability of microlensing increases with the velocity dispersion to the fourth power, and the large number of elliptical hosts is therefore consistent with lensing. Furthermore, a few BL Lacs have been found with emission line redshifts differing from the absorption line redshifts of their host galaxies (Stickel, Fried & Kühr 1989) as predicted by this model. Other authors, however (Narayan & Schneider 1990; Gear 1991), have suggested

that the single images in these candidate microlensed objects are difficult to reconcile with the Ostriker & Vietri model, either because the lensing galaxy would have to be very underdense, or because the geometry of the situation would also involve macrolensing, which would multiply distort the images. Gear (1991) has also pointed out that multiwaveband monitoring of the spectra of BL Lacs and OVV quasars implies that the continuum emitting regions of OVV quasars are much too large to be lensed by stars.

High resolution optical imaging of BL Lac host galaxies is a powerful test of both beaming and lensing models. Previous work on quasars (Malkan *et al.* 1984; Smith *et al.* 1986; Hutchings 1987; Hutchings & Crampton 1990; Véron-Cetty & Woltjer 1990) suggests that the predicted elliptical host population in the beaming models could be differentiated from disc hosts out to redshifts of $z > 0.3$. Imaging also allows a direct test of one of the prime predictions of the lensing model: that the bright cores of BL Lacs are not centred on their underlying hosts (Ostriker & Vietri 1985). We have therefore recently obtained observations of 23 BL Lacs with the 4.2-m William Herschel Telescope on La Palma. The objects observed were mostly taken from the compendium of BL Lac objects published by Burbidge & Hewitt (1987), along with several X-ray selected objects recently identified in the *Uhuru* (Forman *et al.* 1978; Remillard *et al.* 1989) and Einstein Medium Sensitivity Survey (EMSS) catalogues (Maccacaro *et al.* 1989). Fourteen of these objects were resolved by our observations, with six being sufficiently well resolved to allow morphological classification as elliptical or disc systems.

2 OBSERVATIONS AND DATA REDUCTION

Observations were made during 1989 April 10–12 and 1989 November 29–30 using the William Herschel Telescope (operating at $f/4$ via the Taurus optical system) and a 400×590 GEC P8603 CCD detector (readout noise of 5–10 ADU, ~ 1 electron ADU $^{-1}$, dark count < 1 ADU pixel $^{-1}$ hr $^{-1}$). The image scale was 0.27 arcsec pixel $^{-1}$. All objects were imaged through a Kitt Peak *R*-band filter.

An initial short exposure was made with the telescope centred on the published BL Lac object position in order to identify the object. After this initial exposure, the telescope was moved, if necessary, in order to accommodate a reasonably bright comparison star in the field of view. The final image for each object is the sum of several (typically ~ 5) co-added integrations, with integration times for individual frames chosen to avoid saturation of the BL Lac or comparison star. Guiding was sufficiently accurate to allow most frames to be co-added directly, with re-registration being necessary only for a few objects. Flux calibrations for both runs were performed by observing standard stars several times during each night. Conditions were photometric, with excellent seeing, for most objects. Slight systematic variations in the object fluxes were detected in some of the individual frames for OQ530, while a much larger effect was found in all of the individual frames for ON325, leading us to suspect that these objects were observed through a thin layer of haze. We have corrected for this effect in OQ530 by normalizing the affected frames, and conclusions about the morphology of the host underlying OQ530 are unaffected (star images on the frames are undistorted, and flat-fielding is barely

affected). We cannot, however, exclude the possibility of systematic errors of up to half a magnitude in our photometry of this object. We were unable to correct for the much larger variations in the ON325 frames, and our analysis of this object is therefore rather limited.

With the exception of bright, well-studied BL Lacs such as MKN 501 and AP Lib (which were included as ‘controls’ to verify our photometry), total exposure times were between 1000 and 2000 s per object. Individual frames were debiased and flat-fielded in the standard manner prior to being co-added, using twilight sky exposures as flat fields for all BL Lacs observed in the April run. For several BL Lacs observed during the November run, we improved our flat fielding by displacing the telescope by a few arcseconds prior to each individual exposure, and then median-comparing the resulting CCD frames to generate a flat. This typically reduced the level of residual background ‘structure’ resulting from imperfect flat fielding from around 1 per cent of the background level to less than 0.5 per cent.

A log of observations is given in Table 1.

3 ANALYSIS

3.1 Surface brightness profiles

Surface brightness profiles for the BL Lac and comparison star were obtained using software written by R. Jedzrejewski (Jedzrejewski 1987) as a complement to the *GASP* package developed by M. Cawson (Cawson 1983). This profile-fitting software extracts the surface brightness profiles from the best-fitting elliptical isophotes of the images. For each image, the program returns the surface brightness at a given major axis radius, ellipticity and position axis of the isophote, position shift of the isophote relative to the central isophote, and higher order error terms indicating the accuracy with which the given isophote is fitted by the ellipse. In the surface brightness profiles presented in Fig. 1, only those points whose higher order terms indicated good fits to ellipses are plotted and used in subsequent fits to various galaxy models. We define a ‘good fitting’ isophote to be one where the first four coefficients of the Fourier series describing the residuals around a best-fitting ellipse are all less than 4 per cent of the RMS scatter around the isophote. We were typically able to extract profiles down to ~ 1 –2 per cent of the sky background level. We could of course extract fainter isophotes by relaxing our criteria for good-fitting ellipses, but it was felt that the resulting gain in depth would be offset by the possibility that we would be fitting our galaxy models to low-level morphological disturbances in the hosts (which are unaccounted for in analytical galaxy models), very faint contaminating foreground objects, or spurious structure due to imperfect flat fielding. Obvious obscuring objects on the frames (nearby stars or galaxies or defects on the CCD) were masked prior to the analysis by setting their pixels to a pre-assigned negative value which instructs the software to ignore the masked pixels. The extent to which such masking was necessary for individual BL Lacs is shown in Fig. 1, and will be discussed further in a future paper on the clustering environment of these objects.

The *PROF* software was originally written to extract surface brightness profiles from comparatively large galaxies whose surface brightness gradients are much shallower than the objects we analyse, and relies on a fast bilinear interpolation

Table 1. Record of observations.

Name	RA [1950]	Dec	m_{total}	Date	Exposure [s]	Seeing [Arcsec]
PKS0019+058	00 19 54	05 52 31	> 21	29/11/89	1500	0.8
0300+470	03 00 10	47 04 34	16.3	29/11/89	400	0.8
PKS0422+004	04 22 12	00 29 17	15.4	29/11/89	570	0.6
0503-043	05 03 23	-04 23 16	> 21	29/11/89	1250	0.9
PKS0735+178	07 35 14	17 49 09	16.3	12/4/89	1600	1.1
B20752+258	07 52 35	25 50 37	17.3	12/4/89	1400	1.9
PKS0754+100	07 54 23	10 04 40	16.2	11/4/89	1400	0.9
PKS0808+019	08 08 51	01 55 50	16.2	12/4/89	1700	1.4
PKS0829+046	08 29 11	04 39 51	15.3	11/4/89	1825	1.0
0836+182	08 36 40	18 13 25	16.9	29/11/89	660	0.9
B20912+297	09 12 54	29 45 56	15.7	11/4/89	1500	1.1
4U1057-21	10 57 44	10 05 42	16.1	12/4/89	1600	2.2
MKN180	11 33 30	70 25 00	13.6	11/4/89	500	1.0
ON325	12 15 21	30 23 40	16.7	10/4/89	1500	1.1
1E1402+042	14 02 21	04 16 20	16.5	11/4/89	1600	0.7
PKS1413+135	14 13 34	13 34 18	18.6	11/4/89	1500	0.9
OQ530	14 18 06	54 36 57	15.0	10/4/89	1500	0.9
4U1444+43	14 26 36	42 53 46	15.5	12/4/89	500	1.1
PKS1514+197	15 14 41	19 43 11	16.8	10/4/89	2500	1.1
AP Lib	15 14 45	-24 11 22	14.2	11/4/89	500	1.2
MKN501	16 52 12	39 50 26	12.5	12/4/89	100	0.7
PKS1717+178	17 17 00	17 48 09	17.3	11/4/89	1600	0.7
2335+031	23 35 34	03 10 01	17.8	29/11/89	1430	1.0

Note. Magnitudes listed in column four were obtained by synthetic aperture photometry. Aperture diameters were between 10 and 20 arcsec, and do not enclose all MKN 501, MKN 180, or AP Lib. The seventh column records the full-width at half-maximum of field stars on the CCD frame.

scheme to estimate intermediate pixel values. Experiments we have performed on simulated BL Lacs suggest that a slight improvement in the accuracy of the results could be obtained by adopting a more accurate interpolation routine in the program, but at a great cost in execution time. We therefore decided to retain the bilinear interpolation routine, but to improve upon the resulting accuracy by expanding each image using an accurate but slow multinomial algorithm, prior to running it through the profile fitting software. Tests on simulations indicate that this procedure achieves accuracy comparable to that obtained by incorporating a slower interpolation routine in the profile fitting software, but it is much faster because the slowest interpolations need only be done once.

The resulting surface brightness profiles have errors assigned to individual points by directly sampling the spread of pixel values around a given elliptical isophote. We expect the relative sizes of the error bars on the profiles to be roughly correct using this procedure, but numerical errors and the smoothing inherent in any interpolation make the correct absolute size of the errors uncertain. This does not affect the results of our analysis because we are comparing the *relative* goodness of fit in our data to various models.

This is an important point, since our analysis does not address the much more difficult question of whether or not the (de Vaucouleurs law and exponential law) models universally chosen by workers in the field to characterize underlying galaxies of QSO adequately describe the true morphology of the hosts. Answering this question is complicated not only by the need for absolute errors on each point in the luminosity profile, but also by the fact that the analytic formulae used to model galaxy profiles are generalizations that are rarely followed perfectly, even by nearby galaxies. Furthermore, the underlying hosts of quasars sometimes exhibit morphological disturbances (often attributed to tidal events or mergers) which can alter their luminosity profiles; a similar situation may or may not occur with BL Lacs.

3.2 Modelling

After experimentation with many different models for the surface brightness profiles of stars on our CCD frames, a point spread function (PSF) model given by the sum of a Gaussian and two exponentials was chosen. For observations made under poorer seeing conditions ($\text{FWHM} \geq 1.3$), the second exponential component in this model was found to be

PKS0422+004

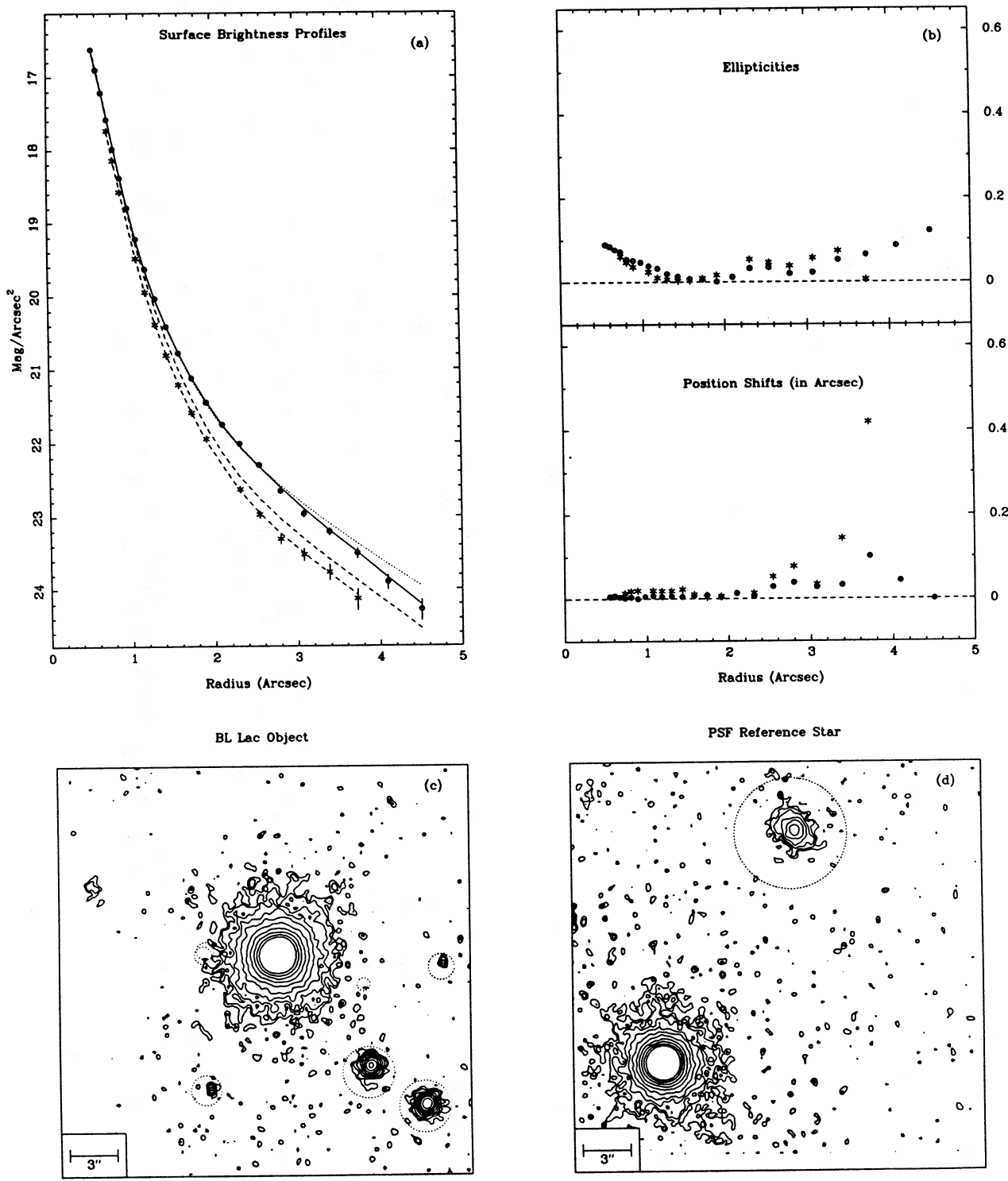


Figure 1. (a) Surface brightness profiles. Points marked by asterisks are the star profile, dots are the BL Lac profile. The dashed line is the best fitting PSF star model (also scaled up to illustrate how well it fits the BL Lac), the solid line is the disc + PSF core model, and the dotted line is the elliptical (de Vaucouleurs law) + PSF core model. (b) Ellipticities and position shifts. Dots represent BL Lac data points, asterisks represent PSF star points. The top curve illustrates the ellipticity of the isophotes as function of semi-major axis radius, while the lower curve records the position shifts of the centres of the isophotes. (c) and (d) Isophotal contour maps of subsections of the CCD frames, showing the resolved BL Lac objects, and their corresponding PSF stars. Lowest contour levels are at 5σ for AP Lib, MKN 501, MKN 180, and 4U 1444 + 43, and at 1.5σ for all other objects. Successive contour levels are displayed logarithmically, and increase in units of $0.5 \text{ mag arcsec}^{-2}$. The areas inside the dotted circles enclose interfering objects excluded from the profile fitting analysis. All objects are centred in these figures, with the exception of the reference stars for PKS 0422 + 004, MKN 180, and PKS 1413 + 135, which were near the edges of the CCD frames and are displayed slightly displaced.

PKS0754+100

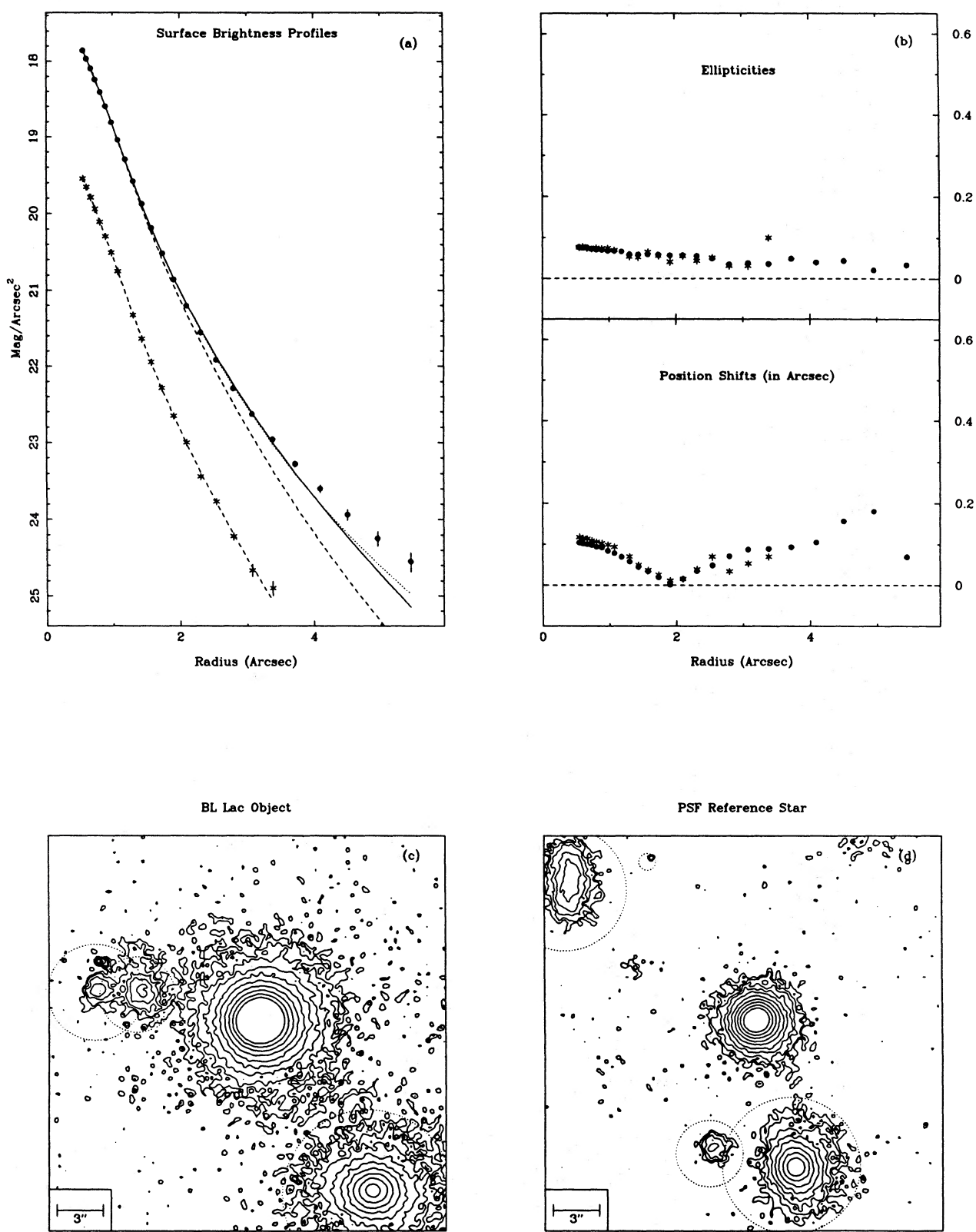


Figure 1 - continued

PKS0829+046

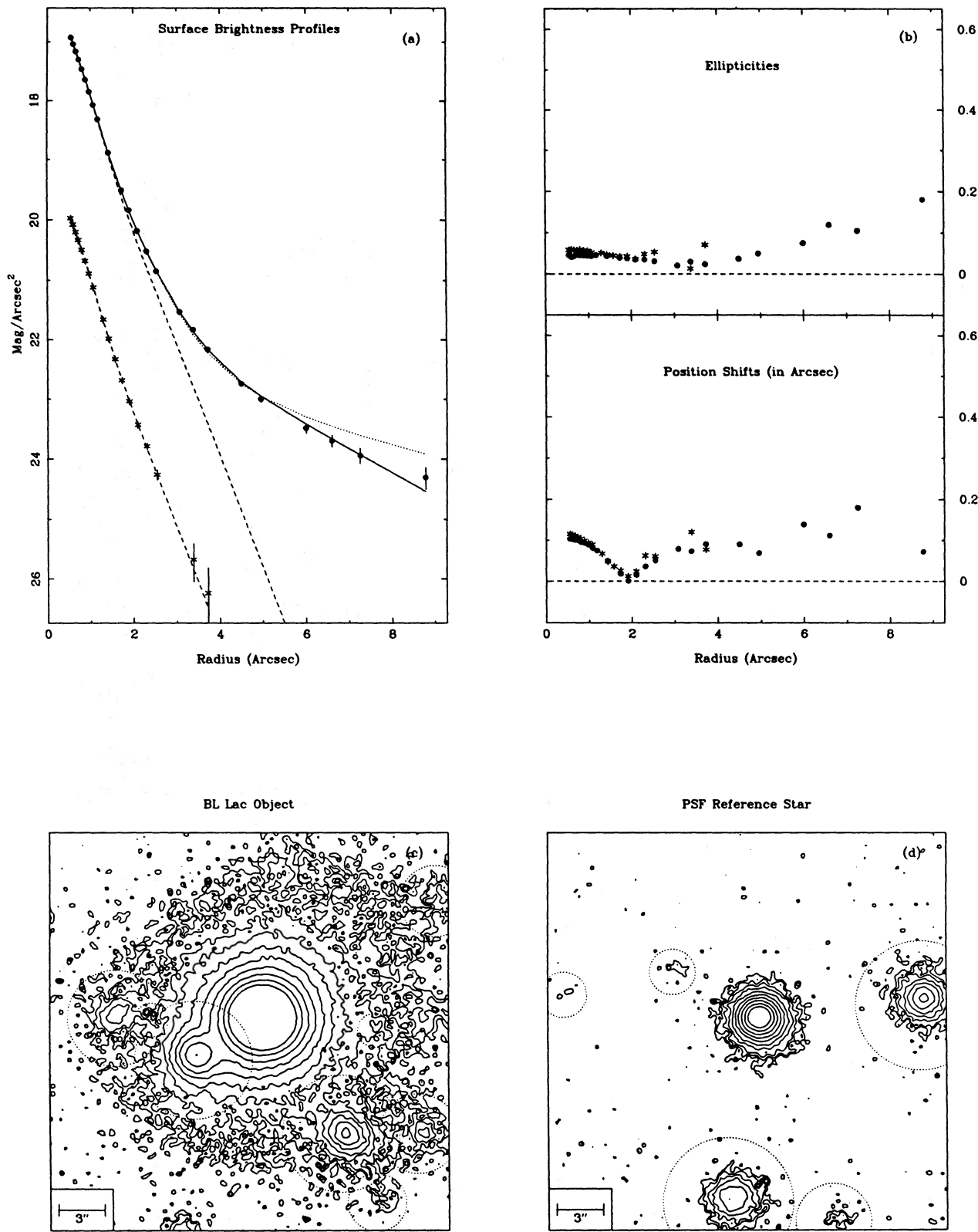
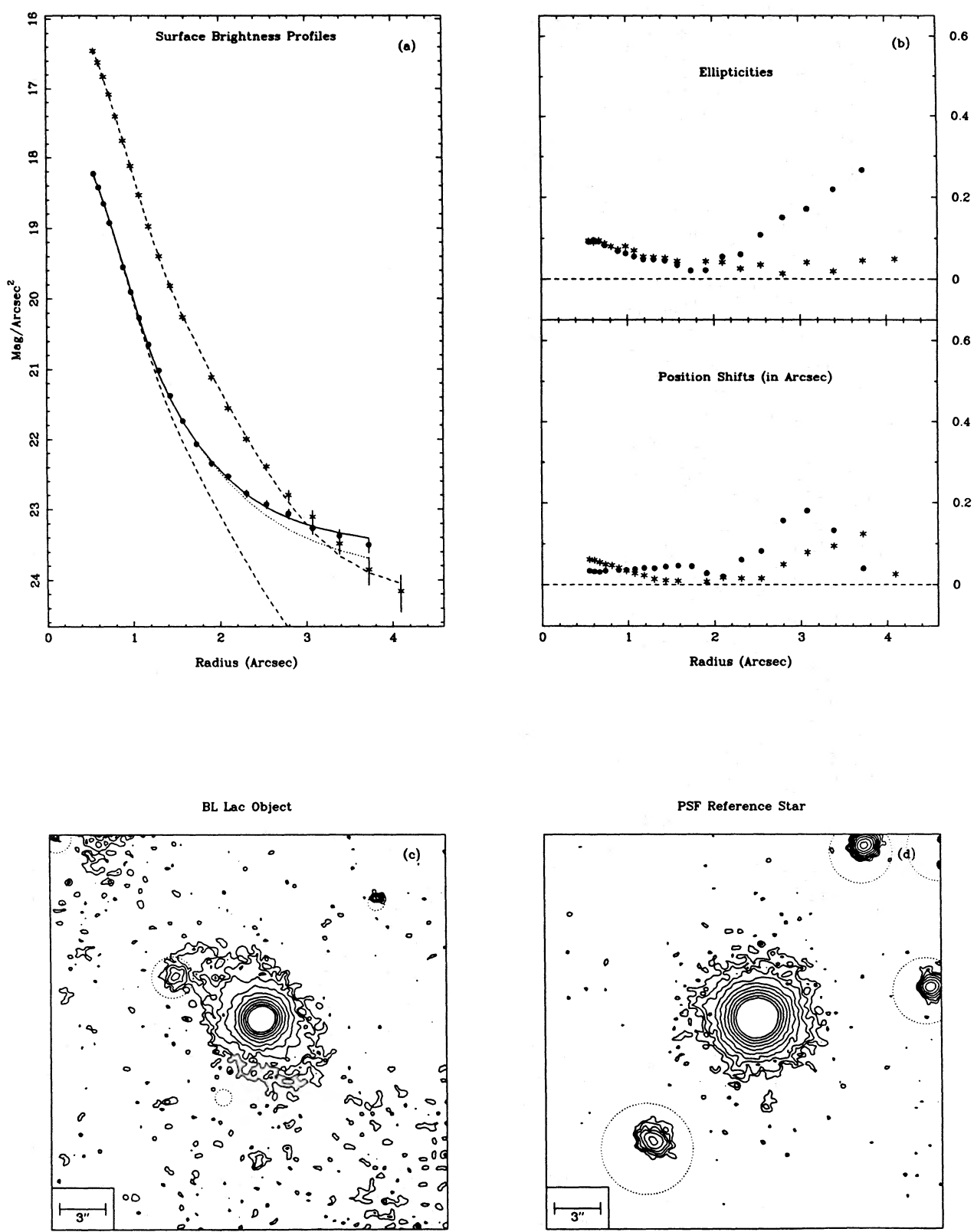


Figure 1 - continued

0836+182

Figure 1 - *continued*

4U1057-21

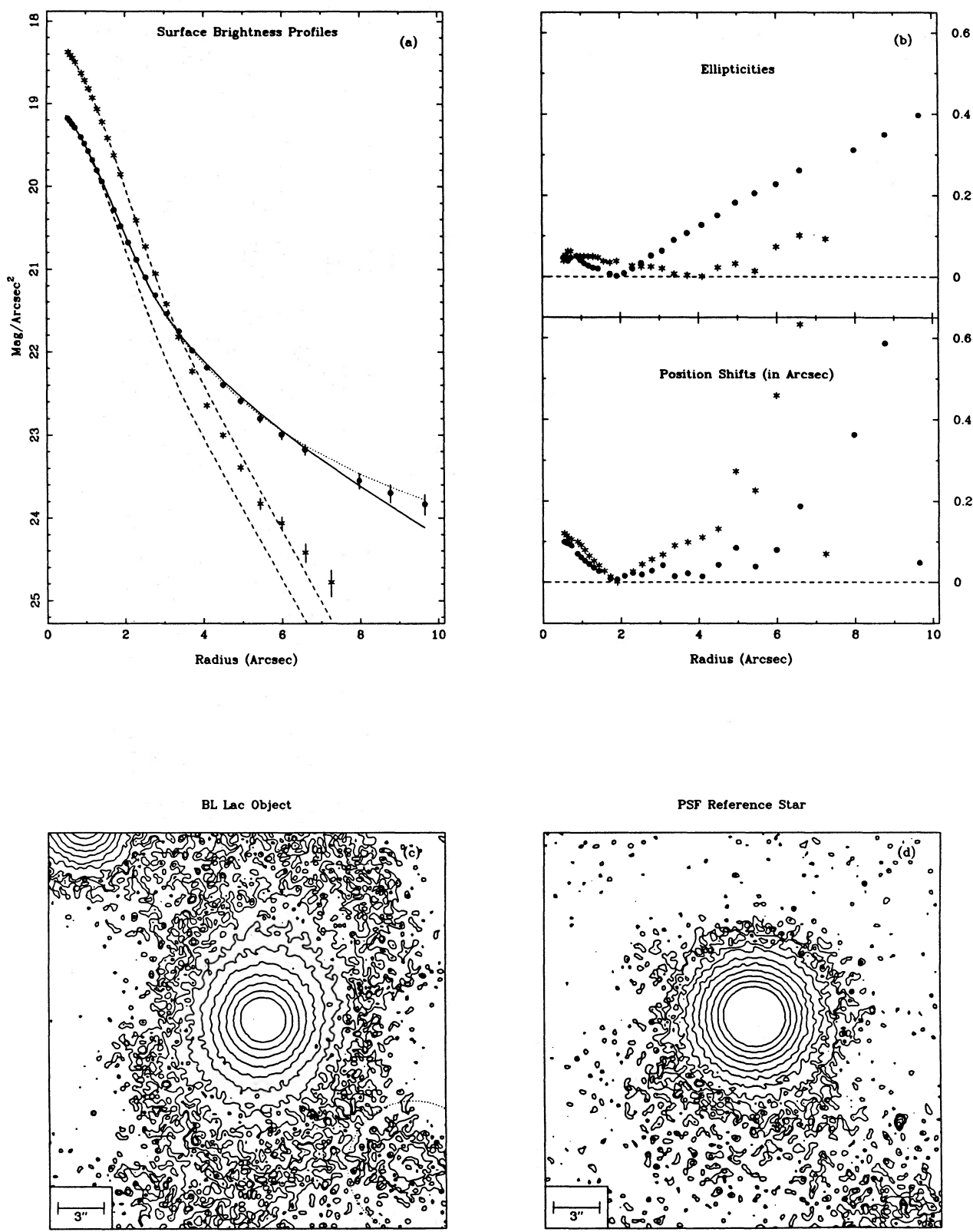
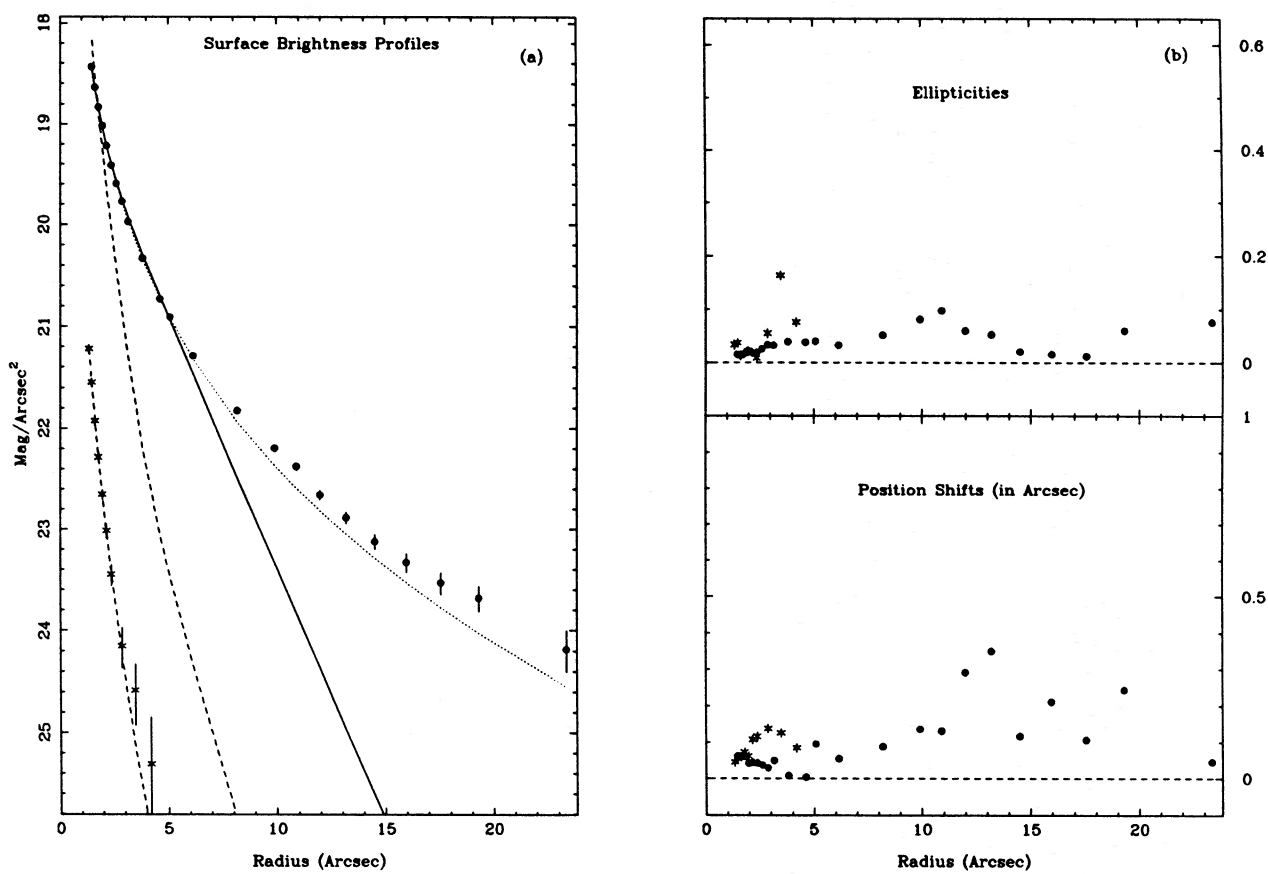
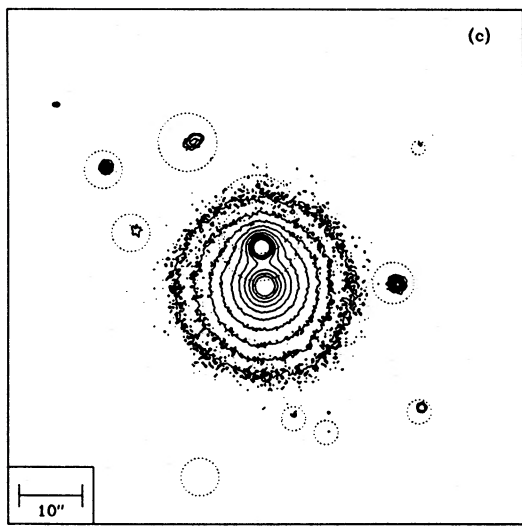


Figure 1 - continued

MKN180



BL Lac Object



PSF Reference Star

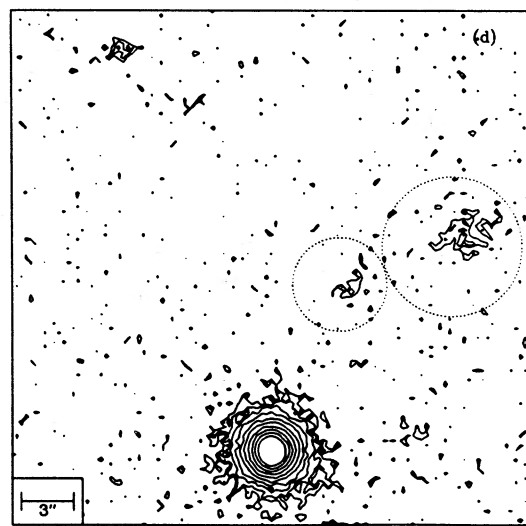


Figure 1 - continued

ON325

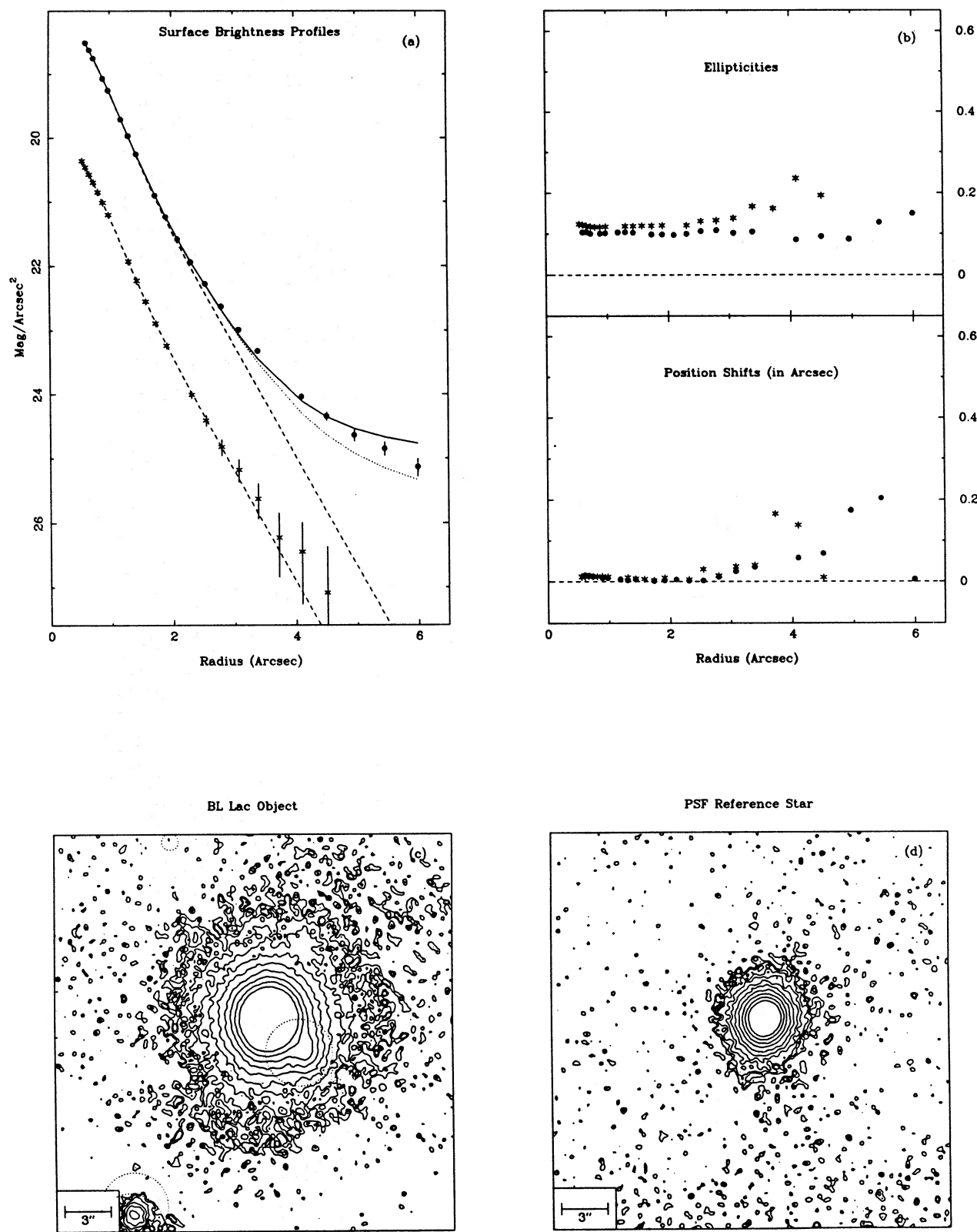


Figure 1 - continued

PKS1413+135

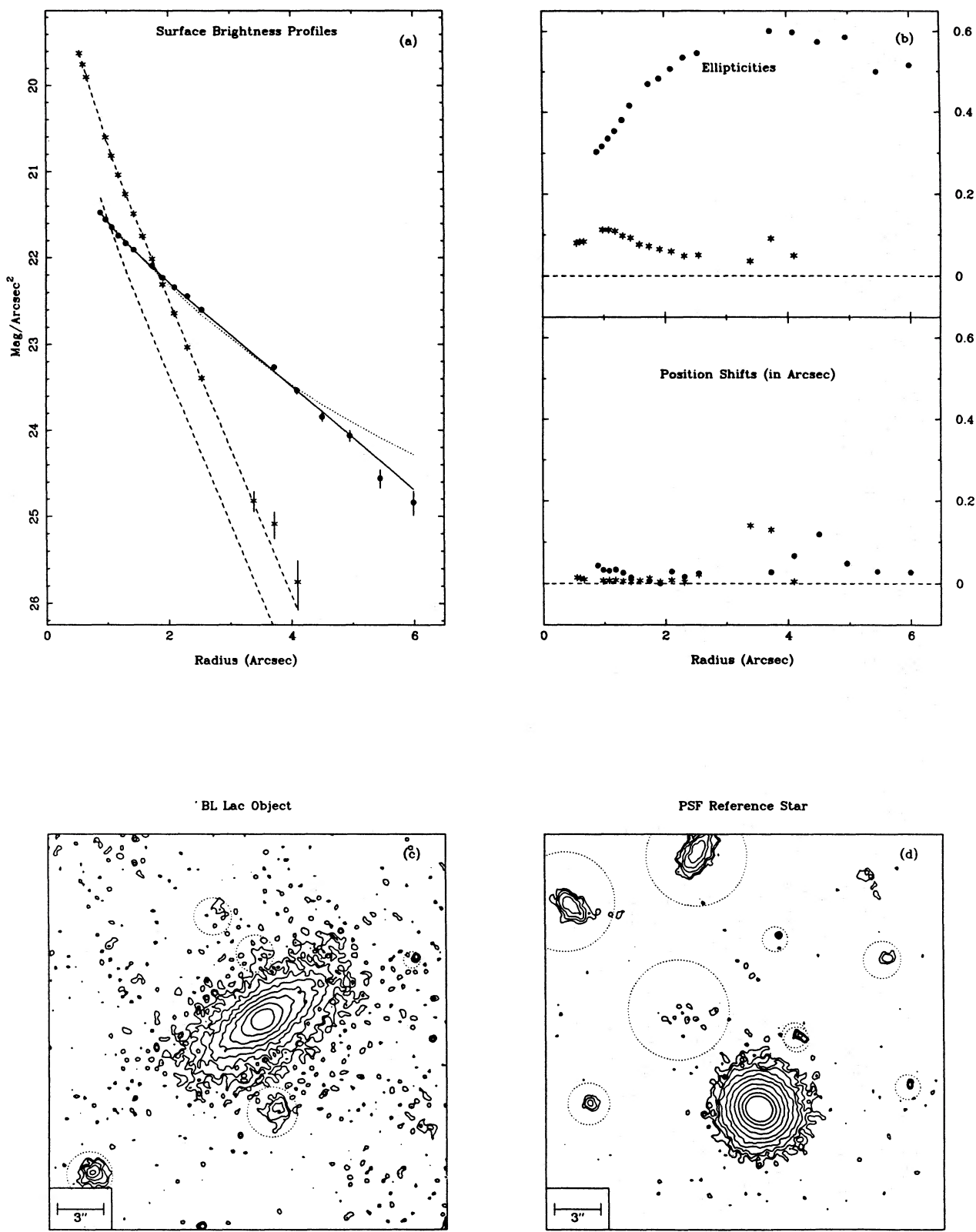
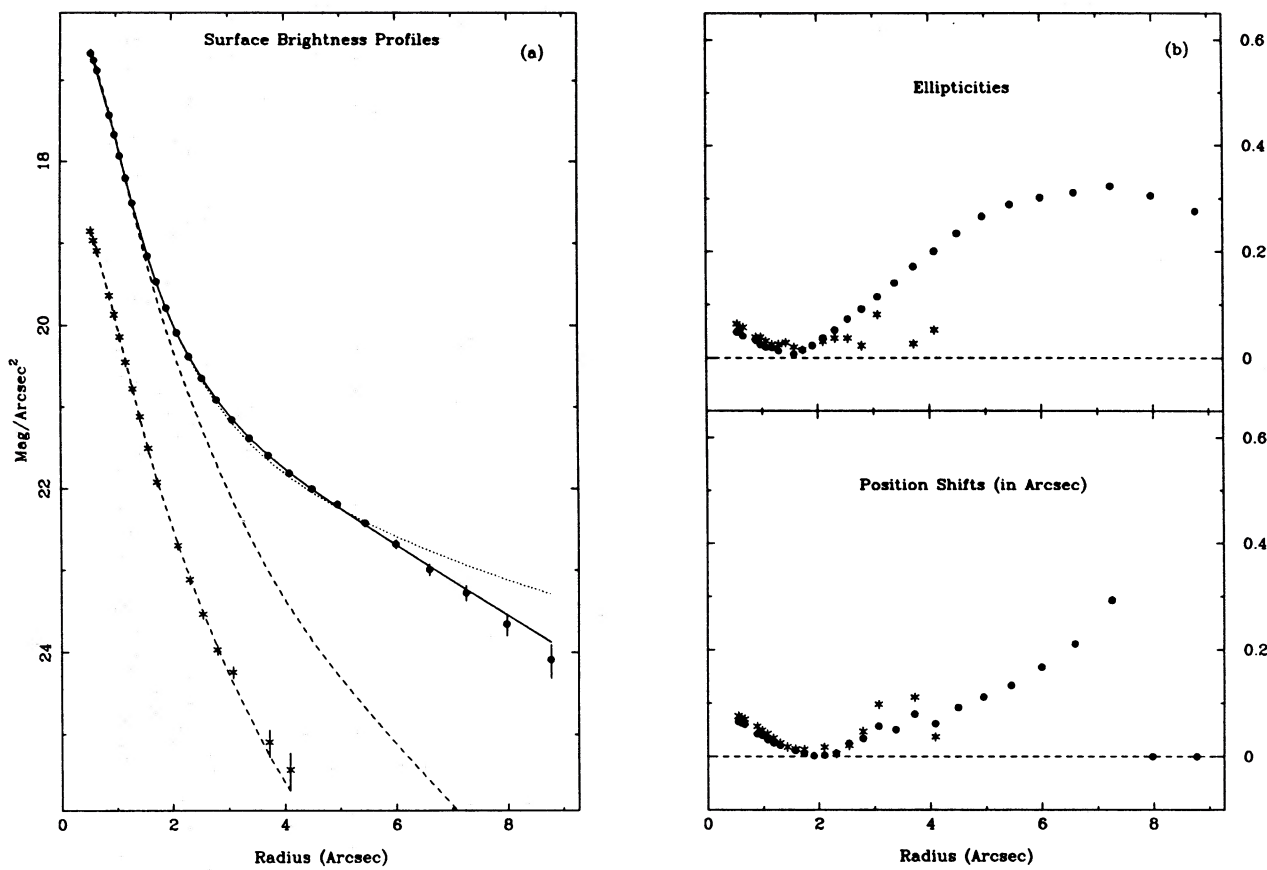
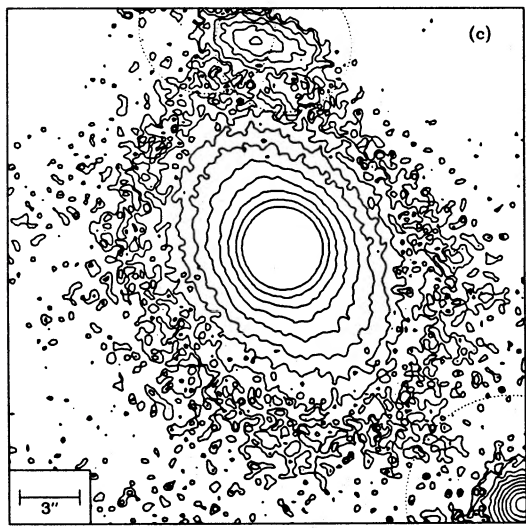


Figure 1 – continued

0Q530



BL Lac Object



PSF Reference Star

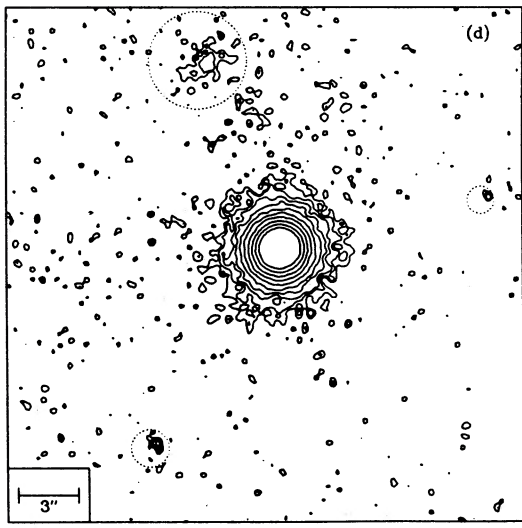
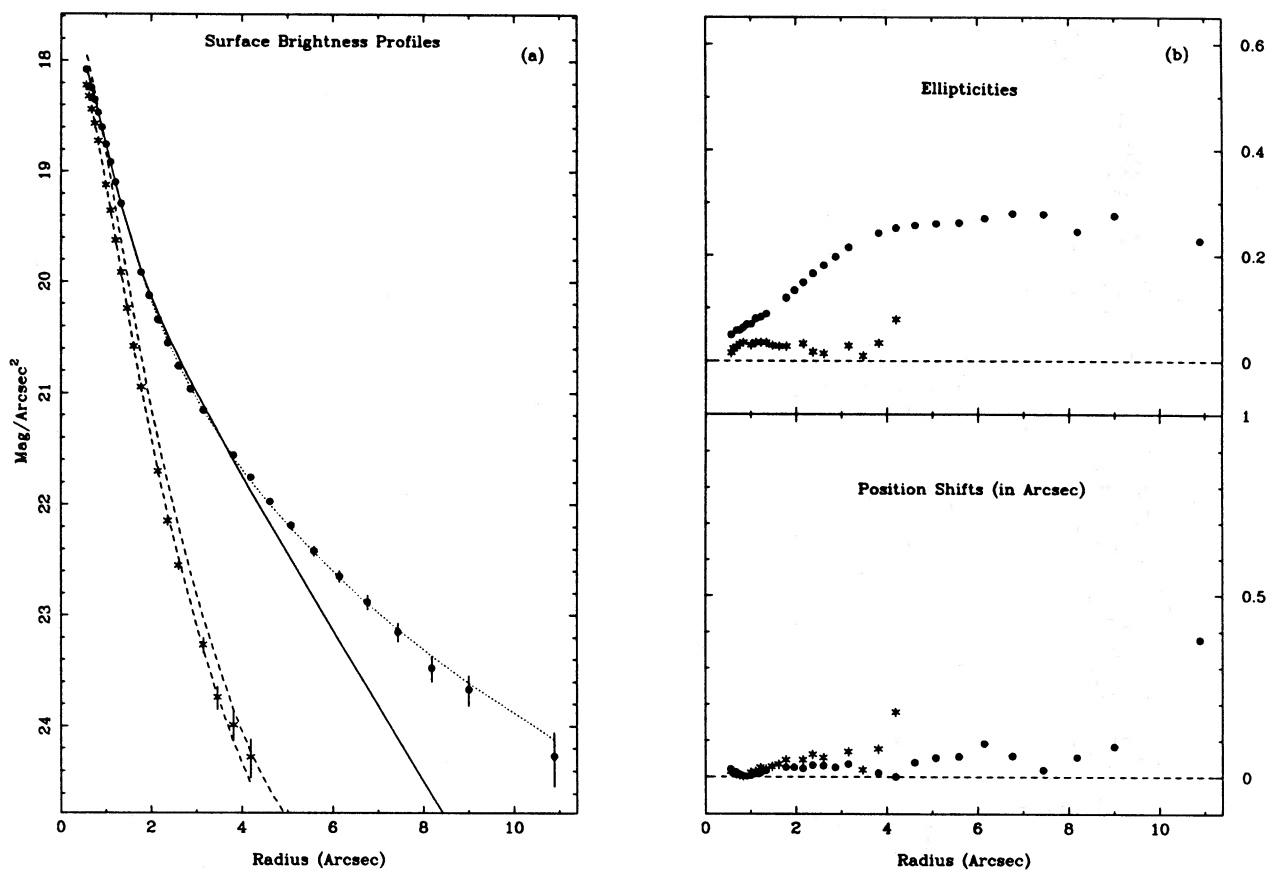
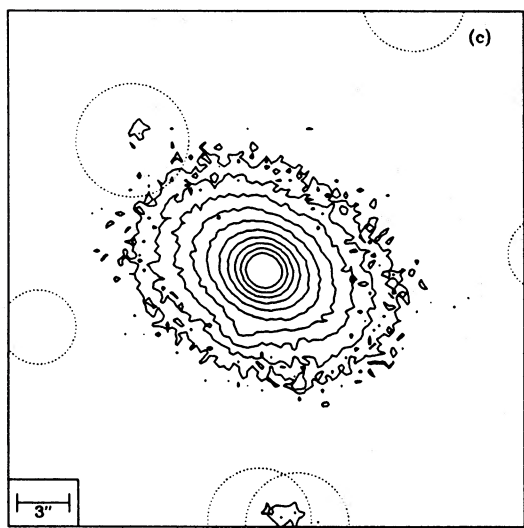


Figure 1 – continued

4U1444



BL Lac Object



PSF Reference Star

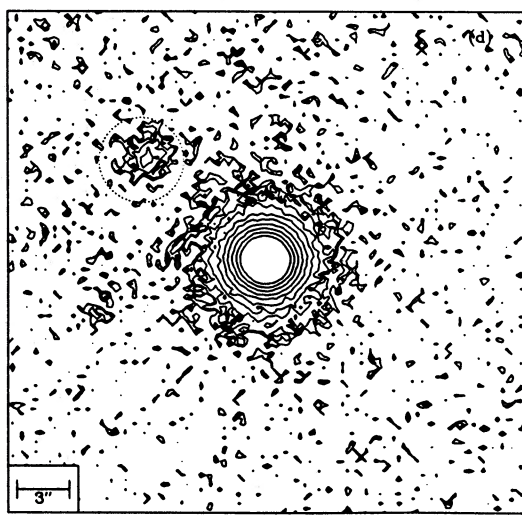


Figure 1 – continued

AP Lib

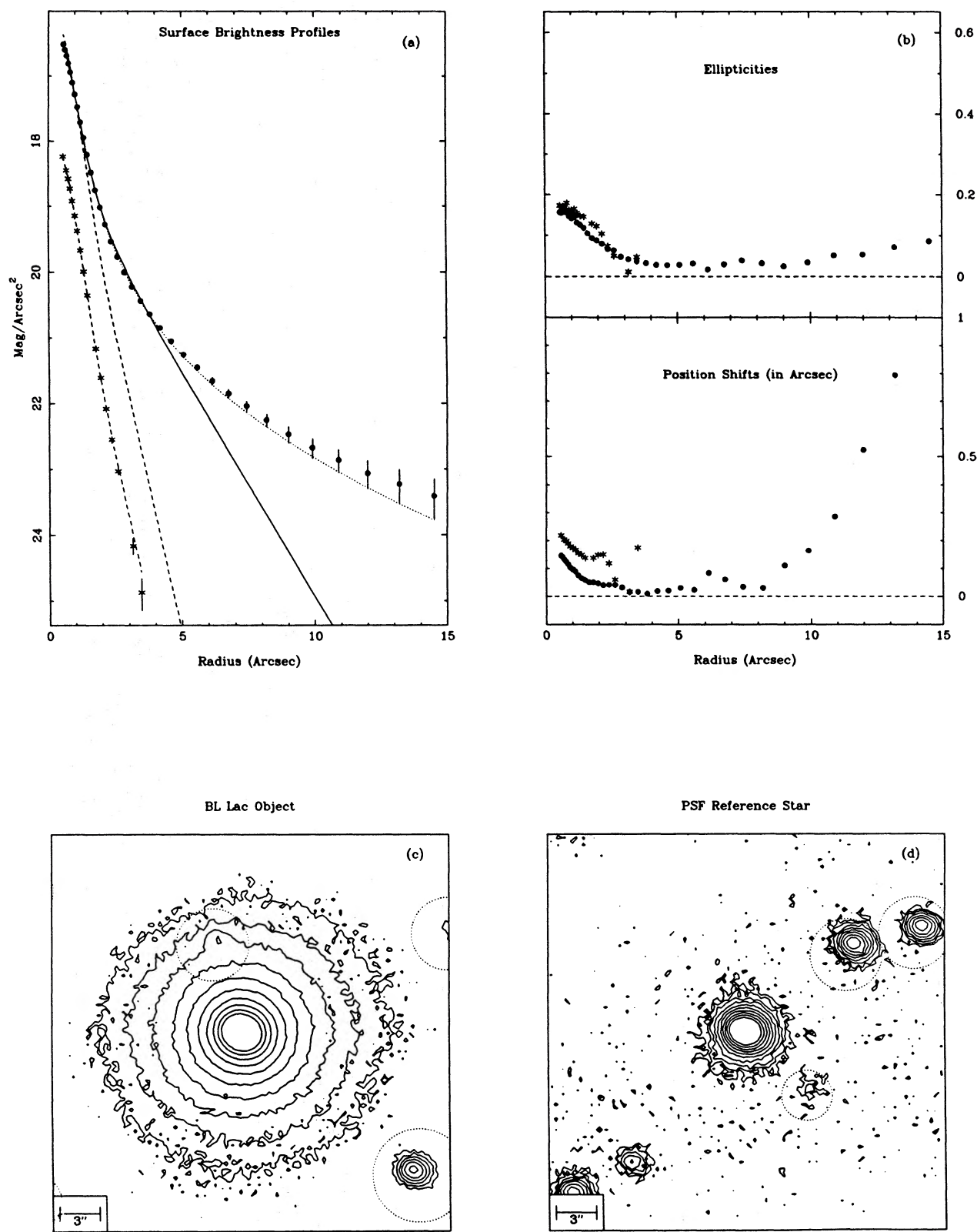
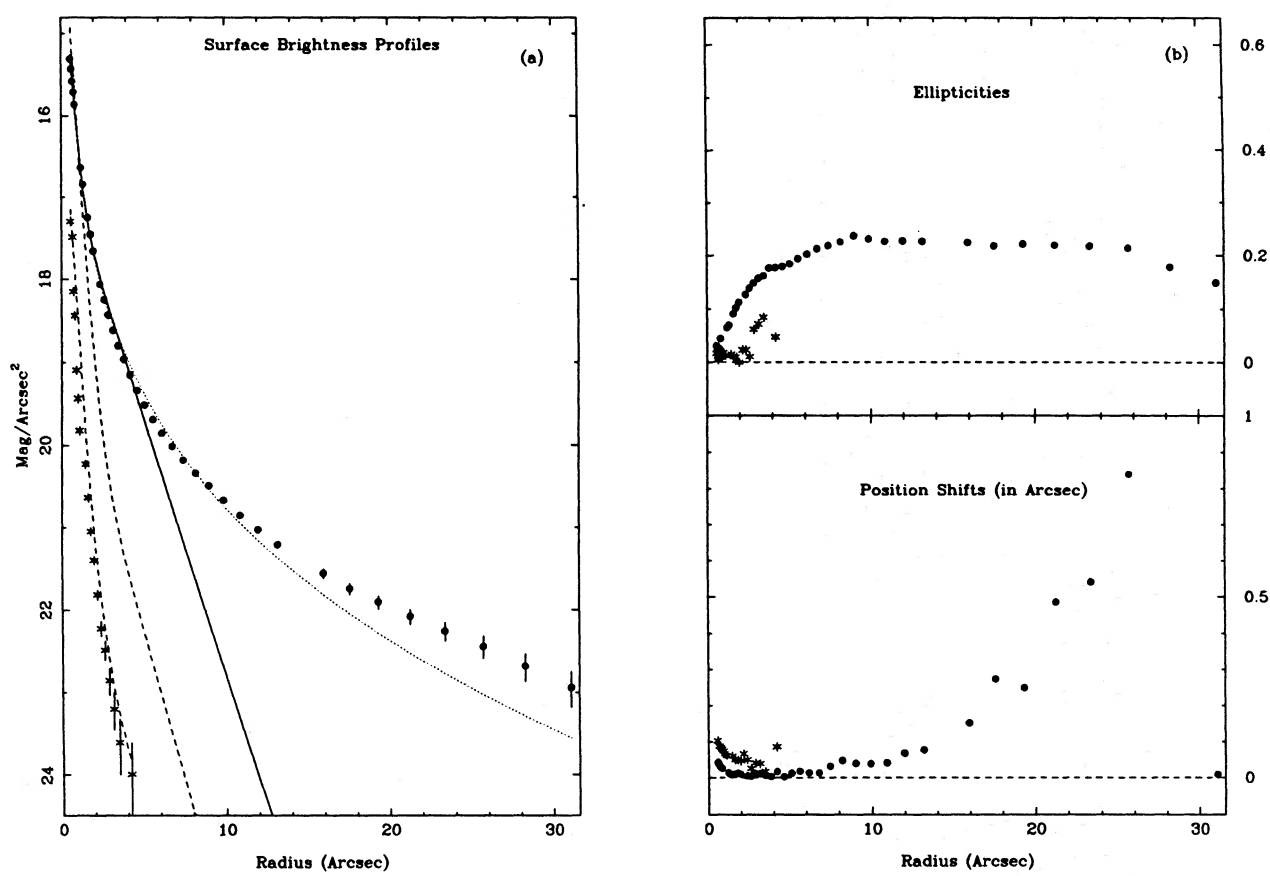
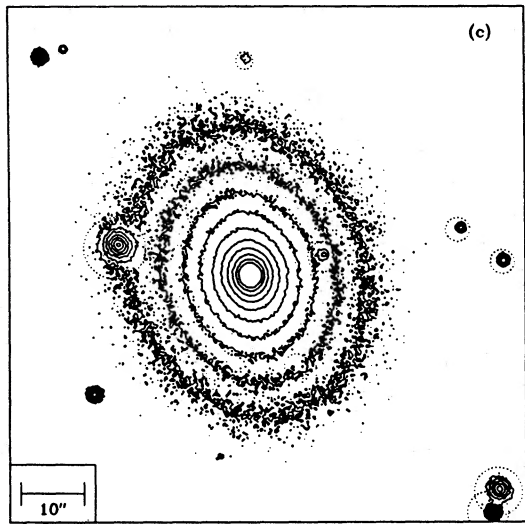


Figure 1 - continued

MKN501



BL Lac Object



PSF Reference Star

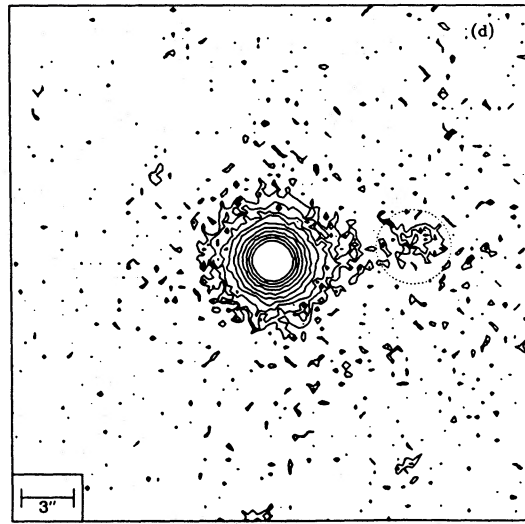


Figure 1 – continued

PKS1717+178

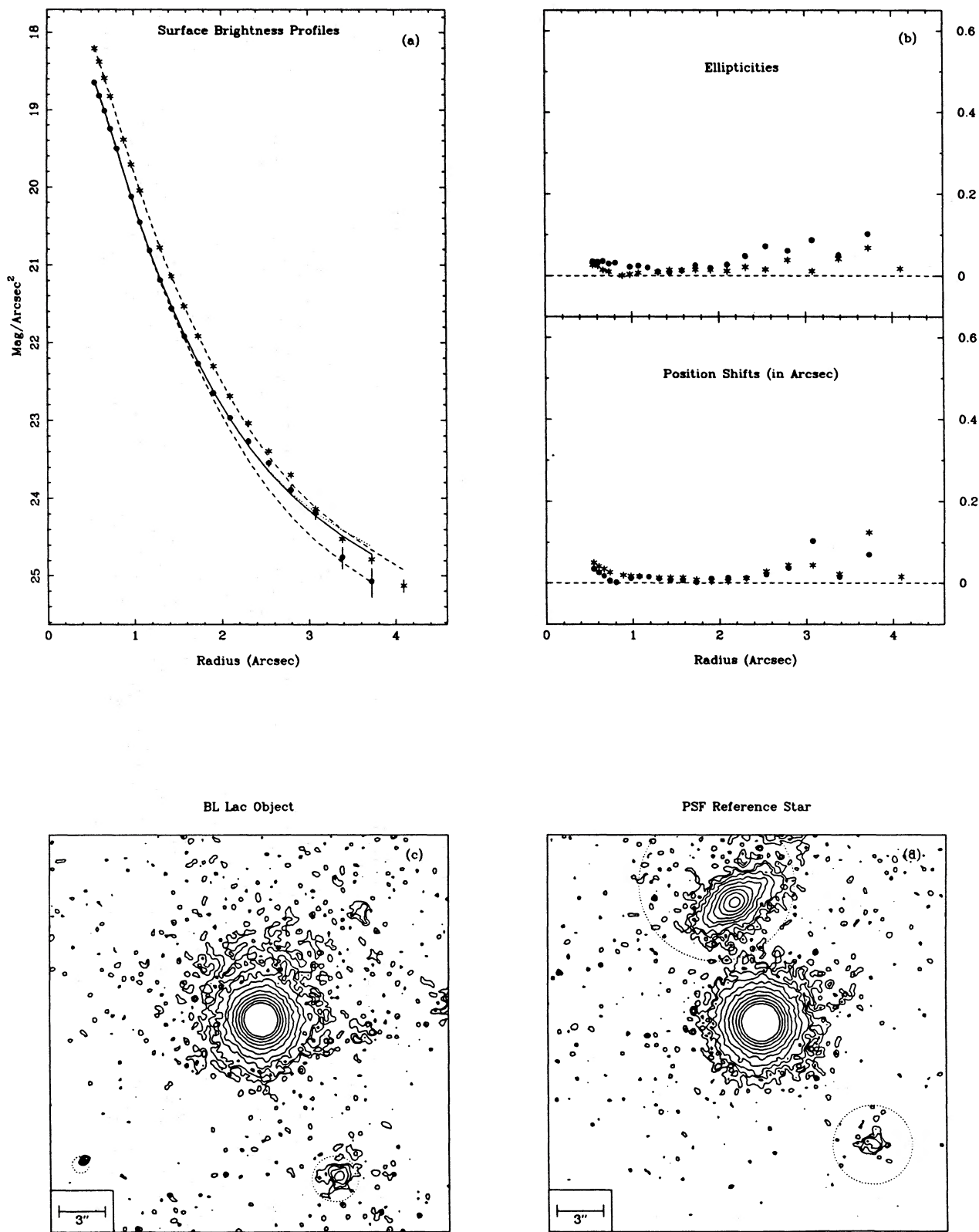
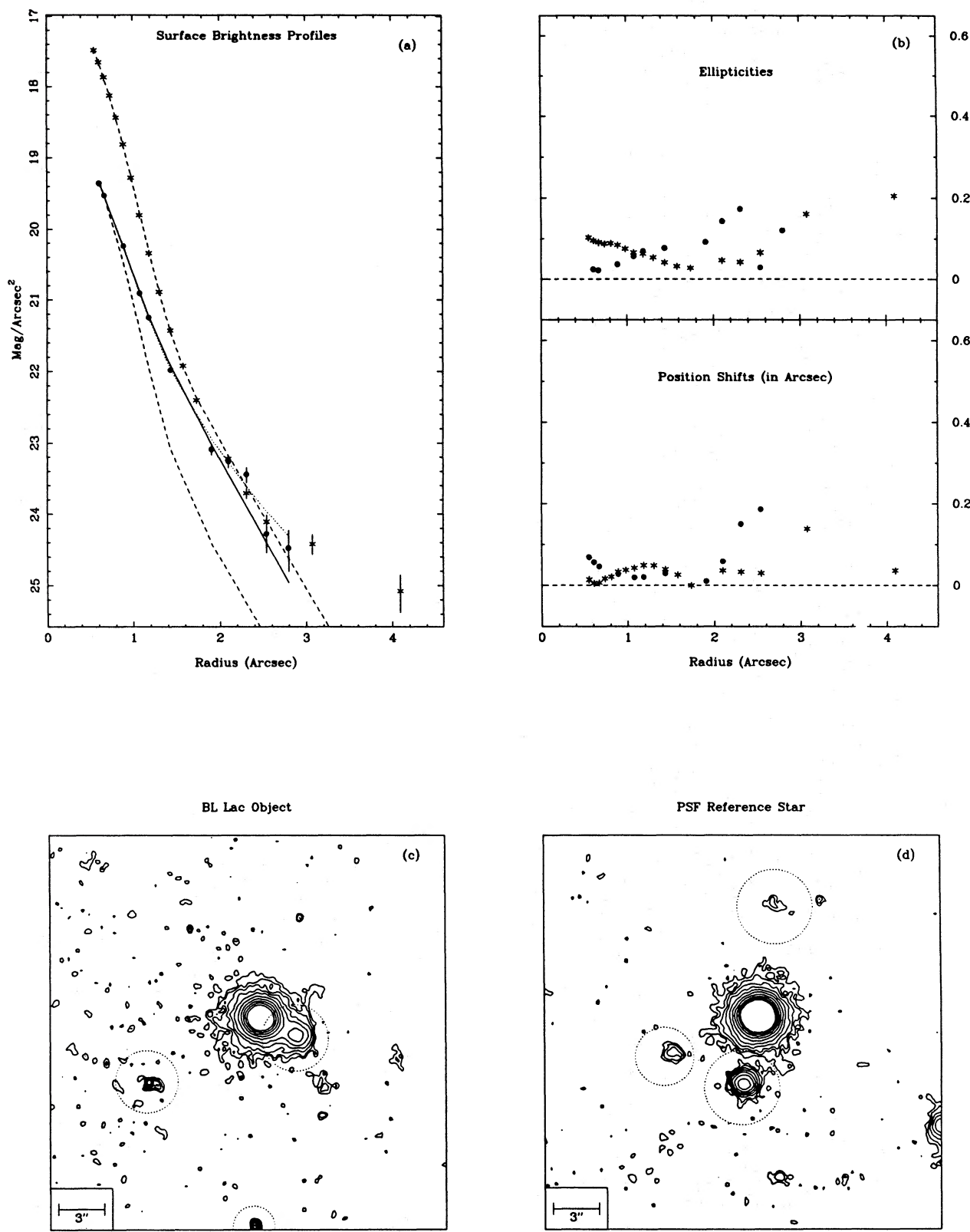


Figure 1 - continued

2335+031

Figure 1 – *continued*

unnecessary. As an aside, we note that the sum of two Gaussians, a model used in the past by a number of authors to model PSF stars imaged by other telescopes, gave much poorer results than our adopted model. Scaled versions of the PSF model were used to describe the BL Lac's central 'point source', and circularly symmetric versions of the PSF were two-dimensionally convolved with galaxy models of specified ellipticity to simulate the effects of seeing. The model fitted to the observed radial profile was the semi-major axis profile of the scaled PSF+convolved galaxy model.

The surface brightness profiles of the BL Lac and host galaxy were modelled as:

- (i) a scaled PSF derived from a star in the CCD frame.
- (ii) a scaled PSF plus a seeing-degraded de Vaucouleurs $r^{1/4}$ law (representing an elliptical host). The undegraded de Vaucouleurs law was defined by

$$\Sigma(r) = \Sigma_e \exp\{-7.67[(r/r_e)^{1/4} - 1]\}$$

where Σ_e is the surface brightness at the effective radius, r_e .

(iii) a scaled PSF plus a seeing-degraded exponential law (representing a disc host). The undegraded exponential model was defined by

$$\Sigma(r) = \Sigma_s \exp(-r/r_s),$$

where Σ_s is the central surface brightness, and r_s is the exponential radius.

Best-fit models were obtained by incorporating the models above into a subroutine, which was then linked into the program QDP (Tennant 1991) as a user-defined function. The free parameters in the fits were the scaling factor for the central point source, and the characteristic radius (r_e for ellipticals, r_s for discs) and characteristic surface brightness of the underlying host (Σ_e for ellipticals, Σ_s for discs). QDP does the fitting using a modified version of the CURFIT subroutine given in Bevington (1969).

Sky backgrounds were sampled in regions near the BL Lac and comparison star, and the modal background values were incorporated as fixed parameters in the fits. Standard deviations of the modal sky values in the sampled regions were added in quadrature to the errors assigned by the profile extraction software in order to account for uncertainty in background values. Classification into a given morphological type was based upon the results of an F-test on the relative χ^2 values returned by the fits. An F-test was first performed comparing the relative χ^2 values of the PSF BL Lac model to the PSF+host BL Lac models. A successful host detection at this stage corresponded to an F-test result indicating statistically significant improvement in the fit, resulting from the inclusion of host components, at a 90 per cent confidence level. At this stage the statistically significant 'detection' of a host underlying B20912+297 was rejected because its reference star was much fainter than the BL Lac, and we could not be certain that this 'detection' was not an artifact resulting from extrapolating the PSF model for the BL Lac well beyond the limited reference star data.

If a host was detected, a second F-test was performed comparing the relative χ^2 values of the two host models to each other. The host was classified as a disc or an elliptical if this test indicated that one model was significantly better than the other at a 90 per cent confidence level. If the F-tests

indicated equally good fits, we classified the host morphology as 'unknown'. In order to test the reliability of our results for fainter hosts, we applied our analysis technique to a number of synthetic BL Lac models. These simulations indicated that we could reliably differentiate between disc and elliptical hosts out to redshifts of $z > 0.3$ for hosts with $M_V \sim -22$ and faint ($m_r \sim 18$) cores.

In obtaining best fit models for the BL Lacs, the galaxy model surface brightnesses and scalelengths were allowed to vary independently. No *a priori* attempt was made to restrict the fitted parameters to 'astrophysically reasonable' ranges. In those cases where hosts were detected and the redshift of the object was known, however, the parameters for the best fitting models did fall into a range consistent with the parameters of normal bright galaxies (our criteria for 'normal bright galaxies' are discussed at length in Section 4.3 below). The parameters for the rejected host model were generally outside this range. We view this as a useful check on the consistency of our results, but emphasize that our classifications for BL Lac hosts are based entirely on the relative χ^2 of the fits, and not on our preconceptions about reasonable values for the fitted parameters.

Where a host was detected but disc and elliptical models gave equally good fits (i.e. those hosts classified as having 'unknown' morphology), one or both of the fitted models usually gave parameters consistent with realistic underlying galaxies. The low signal to noise level of most of these detections implies that many of these 'unknown' morphology hosts are probably quite distant ($z \geq 0.3$), and we consider conclusions drawn from these objects to be much less secure than those obtained from the other objects.

4 RESULTS AND DISCUSSION

Surface brightness profiles for resolved BL Lacs, and the corresponding best fit models, are illustrated in Fig. 1(a). Detailed model fitting results and best fit parameters are given in Table 2. Of the 23 BL Lacs in our sample, eight possessed known redshifts: MKN 501 ($z = 0.0337$), MKN 180 ($z = 0.0458$), AP Lib ($z = 0.0486$), 4U 1444+43 ($z = 0.129$), OQ 530 ($z = 0.152$), 4U 1057-21 ($z = 0.184$), PKS 1413+135 ($z = 0.26$), and PKS 0735+178 ($z = 0.424$). With the exception of PKS 0735+178, all of these were resolved by our survey. Only the hosts underlying MKN 501, MKN 180, AP Lib, and OQ 530 were morphologically classified prior to our survey (all as large ellipticals). We confirm the classifications for MKN 501, AP Lib, and MKN 180, reclassify OQ 530 as a disc, and newly classify the hosts underlying a further two (4U 1444+43 as an elliptical, and PKS 1413+135 as a disc). The two classified disc hosts in this survey are at moderately large redshifts, but were observed under excellent seeing (0.9 arcsec), and are at redshifts where we can securely differentiate ellipticals from discs (compare, for example OQ 530 and 4U 1444+33, which are at similar redshifts).

Of the remaining 15 (presumably most distant) objects in our sample, we were able to resolve an additional seven, none of which we were able to morphologically classify.

Fig. 1(b) records the position shifts and ellipticities of the best-fitting isophotes for the BL Lacs and PSF stars, as a function of semi-major axis length. The ellipticity points allow an estimation of the ellipticity of the underlying host,

Table 2. Summary of model fits.

Name	$\frac{\chi^2_{\text{PSF}}}{\chi^2_{\text{ELL}}}$		$\frac{\chi^2_{\text{DISC}}}{\chi^2_{\text{ELL}}}$		Σ_e [$\frac{\text{mag}}{\text{arcsec}^2}$]	r_e ["]	$m_{\text{elliptical}}$	Σ_s [$\frac{\text{mag}}{\text{arcsec}^2}$]	r_s ["]	m_{disc}	COMMENTS:
	χ^2_{PSF}	χ^2_{ELL}	χ^2_{DISC}	χ^2_{ELL}							
PKS0019+058	(see Notes)		-	-	-	-	-	-	-	-	Too faint for profile fitting.
0300+470	0.93	1.04	-	-	-	-	-	-	-	-	Unresolved.
PKS0422+004	15.4	0.74	23.0	1.98	18.6	20.6	0.93	19.1	-	-	Resolved.
0503-043	(see Notes)		-	-	-	-	-	-	-	-	Too faint for profile fitting.
PKS0735+178	0.4	0.49	-	-	-	-	-	-	-	-	Unresolved; $z=0.424$.
B20752	1.71	0.86	-	-	-	-	-	-	-	-	Unresolved.
PKS0754+100	(see Notes)		-	-	-	-	-	-	-	-	Resolved; both models poor.
PKS0808+019	0.78	1.02	-	-	-	-	-	-	-	-	Unresolved.
PKS0829+046	26.7	0.74	25.7	22.9	16.7	21.1	2.72	17.3	-	-	Resolved; faint PSF star.
0836+182	4.5	0.84	27.9	100	17.0	22.3	7.1	16.7	-	-	Resolved.
B20912+297	(see Notes)		-	-	-	-	-	-	-	-	Faint PSF star.
4U1057-21	55	0.93	26.3	39.4	16.5	21.4	3.8	17.1	$\epsilon \approx 0.2$.	Poor seeing.	
MKN180	1478	19.0	21.7	7.10	14.3	18.5	2.16	14.9	$\epsilon \approx 0.1$.		
ON 325	(see Notes)		-	-	-	-	-	-	-	-	Resolved. Unphotometric.
1E1402+0416	(see Notes)		-	-	-	-	-	-	-	-	Unresolved; faint PSF star.
PKS1413+135	108	0.12	24.0	5.3	18.0	20.9	1.71	18.4	-	-	Disc; $\epsilon \approx 0.6$.
OQ530	46.4	0.57	24.7	18.7	16.6	20.3	2.64	16.8	-	-	Disc; $\epsilon \approx 0.3$.
4U1444+43	2844	31.8	21.89	4.20	15.9	18.86	1.44	16.4	-	-	Elliptical; $\epsilon \approx 0.3$.
PKS1514+197	1.35	1.19	-	-	-	-	-	-	-	-	Unresolved.
AP Lib	1107	13.7	21.6	5.66	14.6	18.17	1.56	15.3	-	-	Elliptical; $\epsilon \approx 0.0$.
MKN501	134	12.6	20.59	9.3	12.7	16.6	1.7	13.7	-	-	Elliptical; $\epsilon \approx 0.25$.
PKS1717+178	3.07	1.01	29.7	52.3	22.1	23.9	1.85	22.1	-	-	Resolved.
2335+031	(see Notes)		-	-	-	-	-	-	-	-	Resolved; both models poor.

Note. Host magnitudes in columns 6 and 9 were obtained by integrating models to $R = 25$ mag arcsec^{-2} . Ellipticity values (ϵ) are recorded in the final column.

while the position shift points test for decentring of the point-like core of the object (which dominates the inner isophotes) from the underlying galaxy (which dominates the outer isophotes). None of the objects in our sample exhibit evidence for decentring, although our method is probably not sensitive to very small decentring on scales of less than 0.5 arcsec.

While our morphological classifications are based purely upon χ^2 results from the model fits, we emphasize that these classifications are consistent with the immediate impression given by inspection of both the images and surface brightness profiles. The high ellipticity in PKS 1413 + 135 is suggestive of a disc host. Similarly, simple morphological classifications can be made by inspection of the profiles for some of the more extended hosts (e.g. AP Lib, 4U 1444 + 43, OQ 530, PKS 1413 + 135), since the fit to the PSF models allows a determination of the limiting radius inside which the signal from the central point source is dominant (typically ~ 3 arcsec). The expected morphological classification is clear from the remainder of the profile, with de Vaucouleurs law ellipticals turning up at large radii, while those objects classified as discs have profiles that remain straight, or even turn slightly down. These simple classifications agree perfectly with the detailed fit results.

The previous classification of OQ 530 as an elliptical

(Stickel *et al.* 1991) was not based upon a full deconvolution of the point source and galaxy components, but rather on an unconvolved fit of galaxy models to the outer portion ($r > 5$ arcsec) of the visible host galaxy (which extends out to $r \sim 9$ arcsec). By adopting the effective radius given in Stickel *et al.* (1991), we also obtain a good fit to an elliptical galaxy profile in these outermost regions (although a disc model gives a similarly good fit), but the resulting seeing-convolved elliptical galaxy model *alone* exceeds the surface brightness of the observed BL Lac (combined galaxy + core) between $2 < r < 5$ arcsec, clearly ruling out this model. The point source in OQ 530 appears to have been ~ 0.5 mag brighter during Stickel *et al.*'s observation of OQ 530, possibly masking this effect. In our opinion, successful morphological classification of objects at these redshifts crucially depends upon careful modelling of the point spread function, and upon its subsequent incorporation into model fits.

4.1 Implication of BL Lacertae disc host galaxies for unified schemes

The most remarkable aspect of our survey is the discovery of disc hosts underlying three BL Lacs. Previously, Halpern *et al.* (1986) claimed to have resolved an underlying disc host

in 1415.6 + 2557, but this isolated observation did not receive sufficient attention to seriously question the validity of simple beaming models. More recently, Stickel, Fied & Kühr (1988) have reported the existence of a disc host in the lens candidate 0537 – 441, and Falomo (1991) has reported the discovery of pointed isophotes in H2356 – 309 (4U 0009 – 33), suggestive of a weak disc underlying the dominant elliptical structure in this object. In a separate paper (McHardy *et al.* 1991) we have described in more detail our discovery of the disc system underlying PKS 1413 + 135 (also included here as part of our larger survey), adding additional weight to the conclusion that some BL Lacs reside in disc galaxies. The discovery of the additional underlying disc galaxies reported in this paper increases the total number of known disc hosts to four out of the 20 or so classified BL Lac hosts. This poses a serious challenge to the beaming models. While the presence of BL Lac disc hosts is not consistent with the simplest beaming models, the underlying discs we observe are centred on their bright BL Lac cores, and therefore pose a problem for lensing models as well.

With the exception of PKS 1413 + 135, our current images are not of sufficient quality to allow us to separate the central point core from the bulge component of disc BL Lac hosts. For PKS 1413 + 135, we were successful in doing this (McHardy *et al.* 1991), and have classified this object as an S0b – c galaxy under the DDO system. Further imaging is needed to determine the exact classifications of the other disc hosts. There is some precedent for at least moderately strong radio sources being associated with S0 galaxies (Sadler, Jenkins & Kotanyi 1989), and unified scheme models would therefore seem compatible with these hosts, provided examples of collimated beaming in other S0 systems could be found. Unified schemes would have more difficulty if these objects turned out to be late type spirals. We note, however, that disc hosts are also found amongst radio-quiet QSO, leading to unification schemes linking radio-quiet QSO with Seyferts (Weedman 1986). It is possible that our observations are indicative of a closer than expected relationship between BL Lac objects and radio quiet QSO, but the small sample of known BL Lac discs makes comparison difficult. Thus far it appears that the radio-quiet QSO discs are somewhat smaller, and much

bluer, than BL Lac discs (Hutchings, Crampton & Campbell 1984).

4.2 Absolute magnitudes for hosts with redshifts

Absolute magnitudes for BL Lac hosts examined in this survey are given in Table 3, assuming $H_0 = 50 \text{ km s}^{-1} \text{ Mpc}^{-1}$, $q_0 = \frac{1}{2}$, as throughout this paper. In computing these values, we first transformed our Kitt Peak *R*-band colours to the Johnson *V* band by assuming the underlying hosts exhibited a typical old-star spectral energy distribution corresponding to the data in Pickles (1985) and Weedman (1986). We have adopted an old-star spectrum for all objects, including discs, because the two best-studied discs (1415 + 259 and PKS 1413 + 135) both exhibit colours more typical of old stellar populations. Numerical integrations over interpolations of the tabulated values for the spectral energy distribution, modulated by the filter response functions, were used to determine the *K*-corrected colours between observed *R* band (integrated to $\mu_R = 25$ using fitted host parameters) and rest-frame *V* band (integrated to $\mu_V^{\text{rest}} = 26$, assuming no rest-frame *V* – *R* colour gradient in the profiles). We have assumed a typical underlying host ellipticity of 0.2 where we could not measure it directly.

Our derived absolute magnitudes agree well with previously published results for the three control objects included in our sample. Our results differ by less than 0.1 mag with published results for MKN 501 and AP Lib. For MKN 180, the best previously available absolute magnitude determination (Ulrich 1989) could only restrict the host magnitude to within the – 21.8 to – 23.0 range, consistent with our measurement of – 22.8.

For the six morphologically classified objects with redshifts in our sample, we obtain $\langle M_V \rangle = -23.3$, slightly brighter than the value of $\langle M_V \rangle = -22.5$ obtained by Ulrich (1989) in her review of the best available data in the literature for the absolute magnitudes of BL Lac host galaxies, and in good agreement with the value of – 22.9 reported in Stickel *et al.* (1991). This seems consistent with the selection effects inherent in our observations of more distant objects. The disc underlying 1415 + 259 (Halpern *et al.* 1986) is among the brightest of BL Lac hosts, while the remaining discs reported in this paper lie near the centre of the luminosity

Table 3. Absolute magnitudes of host galaxies.

Name	<i>z</i>	Type	<i>F</i>	$m(\mu_V^{\text{rest}} = 26)$	M_V	Comments:
4U1057-21	0.186	Unknown	N/A	≈ 16.0	≈ –24.0	Observed under poor conditions.
MKN180	0.0458	Elliptical	99.9%	14.2	–22.8	–23.0 < M_V < –21.8 (Ulrich 1989)
PKS1413+135	0.26	Disc	99.8%	18.3	–23.3	
OQ530	0.152	Disc	91.0%	16.8	–23.2	
4U1444+43	0.129	Elliptical	99.9%	15.7	–23.9	
AP Lib	0.049	Elliptical	99.9%	14.3	–22.8	$M_V = -22.8$ (Ulrich 1989)
MKN501	0.034	Elliptical	99.9%	12.7	–23.6	$M_V = -23.6$ (Ulrich 1989)

Note. Column 4 is the F-test confidence level for the chosen model. Column 5 records the *R*-band magnitude of the chosen model, integrated out to a radius corresponding to $V = 26$ mag arcsec^{-2} in the object's rest frame. The absolute magnitudes in column 6 have been corrected for extinction (Burstein & Heiles 1978).

sity distribution for BL Lac hosts. It is clear that many more redshifts for BL Lacs are required to determine whether disc and elliptical hosts have different luminosity functions.

The absolute magnitudes determined by this survey remain consistent with the hypothesis that the BL Lac parent population is made up of FR type I radio galaxies, although the discovery of disc hosts is a serious challenge to this model. One possibility is that a hitherto undiscovered population of disc FR type I radio galaxies exists. An imaging survey designed to compare optical properties of FR I and FR II radio galaxies with $z \leq 0.2$ was recently completed by Owen & Laing (1989). They fitted images to a de Vaucouleurs $r^{1/4}$ law to test for ordinary ellipticals, and to a power-law to determine if the galaxies could be better characterized as cD galaxies. They found that while FR I optical light profiles tended to be flatter than FR II profiles, most FR I galaxies were still better fitted by $r^{1/4}$ laws. No attempt was made to fit disc models to galaxies in their survey, but exponential discs would probably be better fitted to $r^{1/4}$ laws rather than to the even more slowly decaying cD profiles. We consider the possibility of some disc FR I radio galaxies to remain open.

4.3 Estimation of redshifts

The lack of redshifts for many of the objects described in this paper prevents us from deriving absolute magnitudes for most objects. We can, however, crudely estimate their redshifts of the hosts by matching the image parameters returned by our fits to the redshifted properties of normal galaxies. We emphasize that any absolute magnitude calculated from this estimation is fixed to be representative of the class used to make the estimate, and should not be used to test against theoretical models. We do, however, hope that these estimates will help observers in selecting instruments and exposure times for future observations of these objects.

A problem in estimating redshifts lies in deciding exactly what a 'normal' BL Lac host looks like. Owen & Laing (1989) have demonstrated that FR I galaxies, the parent population in the most widely accepted unification model, display a range of optical properties. The FR I galaxies described by Owen & Laing seem optically rather similar in luminosity and morphology to the brightest cluster galaxies studied by a number of observers. We have therefore chosen to adopt them as our 'reference' set of elliptical galaxies for comparison with our BL Lac elliptical host models. A reference set of galaxies for disc model hosts is more difficult to come by, and after some experimentation we decided simply

to define a galaxy that was an amalgamation of the properties of the known BL Lac disc systems, and to use that in the redshift estimates.

4.3.1 Elliptical hosts

We estimate the redshifts of the elliptical hosts by assuming that their central surface brightnesses and effective radii are correlated according to the relationship given by Hoessel & Schneider (1985) for brightest galaxies in Abell clusters. The Hoessel and Schneider relationship gives reasonable agreement when used to predict parameters for the (mostly control) BL Lacs in our sample with known redshifts and elliptical hosts: MKN 180 (predicted $z = 0.059$, true $z = 0.046$), MKN 501 (predicted $z = 0.022$, true $z = 0.034$), AP Lib (predicted $z = 0.067$, true $z = 0.049$), and 4U 1444+43 (predicted $z = 0.106$, true $z = 0.129$). These predicted redshifts are consistent with the ~ 0.75 mag dispersion in the central surface brightnesses of the Hoessel and Schneider relationship. Assuming $q_0 = \frac{1}{2}$, for our sample of ellipticals to obey the Hoessel and Schneider relationship we must numerically solve the following for z :

$$\Sigma_e^{\text{observed}} = 18.82 - 0.365$$

$$+ 3.02 \log \left[r_e \frac{(1+z) - \sqrt{1+z}}{3.44 \times 10^{-4} H_0 (1+z)^2} \right] \\ + 10 \log(1+z) + K(z),$$

where r_e is the observed effective radius in arcseconds, and the second term is the adopted correction between the Thuan and Gunn r band used by Hoessel and Schneider and Kitt Peak R band. The resulting predicted redshifts and absolute magnitudes for the ellipticals in our sample, as well as for those objects with unknown morphologies, are shown in Table 4. Note that the Hoessel and Schneider relationship is calibrated using $H_0 = 60 \text{ km s}^{-1} \text{ Mpc}^{-1}$, and that this value was used in solving the equation above to estimate the redshifts. The effective radii and absolute magnitudes as given in Table 4 have been converted to the $H_0 = 50 \text{ km s}^{-1} \text{ Mpc}^{-1}$, $q_0 = \frac{1}{2}$ system used throughout this paper.

4.3.2 Disc hosts

Little is known about the detailed morphological characteristics of BL Lac disc hosts, and any procedure we adopt to estimate their redshifts is bound to be imprecise. At redshifts large enough to make the newly discovered discs as faint as

Table 4. Estimated absolute magnitudes for host galaxies with unknown morphology.

Name	z Elliptical	z Disc	M_V Elliptical	M_V Disc	COMMENTS:
PKS0422+004	0.31	0.15	-23.6	-20.8	
PKS0829+046	0.25	0.23	-24.8	-23.9	
0836+182	0.28	0.27	-24.8	-25.0	Both models doubtful.
PKS1717+178	No Solution	0.43	N/A	-21.2	No convergence for elliptical.

Note. Columns 2 and 3 give estimated redshifts based upon assumed morphologies (see text). Columns 4 and 5 give the corresponding absolute magnitudes.

we observe them, these systems would have to be quite large, with exponential radii of order 10 kpc. Such radii are consistent with the range of sizes exhibited by the discs underlying 1415.6 + 2557 (17 kpc), PKS 1413 + 295 (9 kpc), and OQ 530 (9 kpc). A simple redshift estimate can be made by assuming a fixed rest-frame size and calculating the redshift at which this would be observed at the apparent size. By adopting an intermediate scale size of 12 kpc, for the known discs we would have estimated $z = 0.48$ for PKS 1413 + 135 (true $z = 0.26$), $z = 0.22$ for OQ 530 (true $z = 0.15$), and $z = 0.15$ for 1415 + 297 (true $z = 0.24$).

We can obtain another estimate by assuming that BL Lac disc hosts exhibit the constant central surface brightness $\mu_B = 21.65$ found by Freeman (1970) in a sample of nearby spirals. By further assuming an old star colour correction (consistent with the old-star colours exhibited by PKS 1413 + 135 and 1415 + 297) of 1.5, we can estimate the redshift at which the $(1+z)^4$ monochromatic flux-dimming and K -correction reduces this central surface brightness to the observed level. This procedure appears, on the whole, to give similar results to the one outlined earlier. Using this procedure we would have estimated $z = 0.19$ for PKS 1413 + 135 (true $z = 0.26$), $z = 0.10$ for OQ 530 (true $z = 0.15$), and $z = 0.28$ for 1415 + 297 (true $z = 0.24$). In any case, the true redshifts tend to be bracketed by the values given by the two procedures, and the values given in Table 4 for the redshifts of the disc hosts are the averages of the two estimates.

4.4 Selection effects in the sample

It is difficult to obtain samples of BL Lac hosts that are complete in any meaningful statistical sense. Few hosts are known, and most published lists of BL Lacs are mixtures of objects selected at different wavelengths. The vast majority of the objects in this sample were radio-selected, and during the course of our observations we became aware of a similar survey being undertaken by Stickel and colleagues of radio selected BL Lacs in the 1 Jy Galaxy Catalogue (Kühr & Schmidt 1990). We tried to minimize overlap with their observations; most of our objects were therefore not in the 1 Jy Catalogue, and we expect our results to be biased towards BL Lacs that are relatively weak in the radio.

It has recently become clear that X-ray selection is a highly efficient tool for discovering BL Lacs (Maccacaro *et al.* 1989). The application of this technique by a number of authors has led to an effective doubling in the number of known BL Lac objects in the last two years. X-ray-selected BL Lacs appear to differ from radio-selected BL Lacs in a number of ways, however. X-ray-selected objects seem to be less variable, less polarized, have flatter overall spectra, and have larger starlight fractions than do radio-selected BL Lacs (Maraschi *et al.* 1986; Ghisellini *et al.* 1986; Stocke *et al.* 1989; Schwartz *et al.* 1989). Authors differ in their assessments of the degree to which these differences are indicative of different populations, as opposed to selection effects resulting from sampling a single parent population with a spread of properties, as suggested by similarities in the extended radio emission exhibited by both classes of objects (Polatidis 1989). Discriminating between these two possibilities is critical if we hope to use the increased numbers of BL Lacs supplied by the X-ray-selected objects in a mea-

ningful way. A comparison of the types of hosts underlying X-ray and radio-selected BL Lacs would enable us to determine if the hosts come from the same population, and would go a long way towards clearing up the issue of whether the X-ray-selected and radio-selected BL Lacs are the same types of objects. We plan to extend our present imaging program to include a number of X-ray-selected BL Lacs.

5 CONCLUSIONS

Our survey of 23 BL Lac objects has resolved many new BL Lac hosts, and we have morphologically classified three of these objects for the first time. No strong evidence for decentring between the BL Lacs and underlying hosts was found in any of these objects. Surprisingly, we have discovered two disc host galaxies, the existence of which is not consistent with standard models for these objects. The ramifications of these observations are still not clear, but the similarity of the absolute magnitudes of these hosts to the FR I radio galaxies suggests that our observations could be indicative of a population of disc galaxies with collimated beaming.

ACKNOWLEDGMENTS

We thank Marie-Helene Ulrich for many useful discussions, Robert Jedzrejewski for the use of his profile fitting software and Brin Cooke for confirming some of our object identifications. We also thank Roger Davies for many helpful suggestions. CSC acknowledges financial support from Balliol College, and RGA acknowledges receipt of an ORS Award. We acknowledge the data analysis facilities provided by the Starlink Project, which is funded by the UK Science and Engineering Research Council. The William Herschel Telescope is operated by the Royal Greenwich Observatory at the Spanish Observatorio del Roque de los Muchachos of the Instituto Astrophysica de Canarias.

REFERENCES

- Barthel, P. D., 1989. *Astrophys. J.*, **336**, 606.
- Bevington, P. R., 1969. *Data Reduction and Error Analysis for the Physical Sciences*, p. 328, McGraw-Hill, New York.
- Blandford, R. D. & Rees, M. J., 1978. *Pittsburgh Conference on BL Lac Objects*, ed. Wolfe, A. M., University of Pittsburgh Press, Pittsburgh.
- Browne, I. W. A., 1983. *Mon. Not. R. astr. Soc.*, **204**, 23P.
- Burbidge, G. & Hewitt, A., 1987. *Astr. J.*, **92**, 1.
- Burstein, D. & Heiles, C., 1978. *Astrophys. J.*, **225**, 40.
- Cawson, M., 1983. *PhD thesis*, Cambridge University.
- Falomo, R., 1991. *Astr. J.*, in press.
- Forman, W., Jones, C., Cominsky, L., Julien, P., Murray, S., Peters, G., Tananbaum, H. & Giacconi, R., 1978. *Astrophys. J. Suppl.*, **38**, 357.
- Freeman, K. C., 1970. *Astrophys. J.*, **160**, 811.
- Gear, W. K., 1991. *Nature*, **349**, 676.
- Ghisellini, G., Maraschi, L., Tanzi, E. & Treves, A., 1986. *Astrophys. J.*, **310**, 317.
- Halpern, J. P., Impey, C. D., Bothun, G. D., Tapia, S., Skillman, E. D., Wilson, A. S. & Meurs, E. J. A., 1986. *Astrophys. J.*, **302**, 711.
- Hoessel, J. G. & Schneider, D. P., 1985. *Astr. J.*, **90**, 1648.
- Hoyle, F., Burbidge, G. R. & Sargent, W. L. W., 1966. *Nature*, **209**, 751.

Hutchings, J. B., Crampton, D. & Campbell, B., 1984. *Astrophys. J.*, **280**, 41.

Hutchings, J. B. & Crampton, D., 1990. *Astr. J.*, **99**, 37.

Hutchings, J. B., 1987. *Astrophys. J.*, **320**, 122.

Jedrzejewski, R. I., 1987. *Mon. Not. R. astr. Soc.*, **226**, 747.

Kühr, H. & Schmidt, G. D., 1990. *Astr. J.*, **99**, 1.

Maccacaro, T., Gioia, I. M., Schild, R., Wolter, A., Morris, S. & Stocke, J., 1989. In: *BL Lac Objects*, p.222, eds Maraschi, L., Maccacaro, T. & Ulrich, M.-H., Springer Verlag, Berlin.

Malkan, M. A., Margon, B. & Chanan, G. A., 1984. *Astrophys. J.*, **280**, 66.

Maraschi, L., Ghissellini, G., Tanzi, E. G. & Treves, A., 1986. *Astrophys. J.*, **310**, 325.

Marscher, A. P. & Gear, W. K., 1985. *Astrophys. J.*, **298**, 114.

McHardy, I. M., Abraham, R. G., Crawford, C. S., Ulrich, M.-H., Mock, P. C. & VanderSpeck, R. K., 1991. *Mon. Not. R. astr. Soc.*, **249**, 742.

Narayan, R. & Schneider, P., 1990. *Mon. Not. R. astr. Soc.*, **243**, 192.

Ostriker, J. P. & Vietri, M., 1985. *Nature*, **318**, 446.

Owen, F. N. & Laing, R. A., 1989. *Mon. Not. R. astr. Soc.*, **238**, 357.

Padovani, P. & Urry, C. M., 1990. *Astrophys. J.*, **356**, 75.

Padovani, P. & Urry, C. M., 1991. *Astrophys. J.*, **368**, 373.

Pickles, A. J., 1985. *Astrophys. J.*, **296**, 340.

Polatidis, A. G., 1989. *MSc thesis*, University of Manchester.

Remillard, R. A., Tuohy, I. R., Brissenden, R. J. V., Buckley, D. A. H., Schwartz, D. A., Feigelson, E. D. & Tapia, S., 1989. *Astrophys. J.*, **345**, 140.

Sadler, E. M., Jenkins, C. R. & Kotanyi, C. G., 1989. *Mon. Not. R. astr. Soc.*, **240**, 591.

Schwartz, D. A., Brissenden, R. J. V., Tuohy, I., Fiegeelson, E. D., Hetz, P. L. & Remillard, R. A., 1989. In: *BL Lac Objects*, eds Maraschi, L., Maccacaro, T. & Ulrich, M.-H., Springer Verlag, Berlin.

Smith, E. P., Heckman, T. M., Bothun, G. D., Romanishin, W. & Balick, B., 1986. *Astrophys. J.*, **306**, 64.

Stickel, M., Fried, J. W. & Kühr, H., 1988. *Astr. Astrophys.*, **206**, L30.

Stickel, M., Fried, J. W. & Kühr, H., 1989. In: *BL Lac Objects*, p. 64., eds Maraschi, L., Maccacaro, T. & Ulrich, M.-H., Springer Verlag, Berlin.

Stickel, M., Padovani, P., Urry, C. M., Fried, J. W. & Kühr, H., 1991. *Astrophys. J.*, in press.

Stocke, J. T., Morris, S. L., Gioia, I. M., Maccacaro, T., Schild, R. & Wolter, A., 1989. In: *BL Lac Objects*, p. 242, eds Maraschi, L., Maccacaro, T. & Ulrich, M.-H., Springer Verlag, Berlin.

Tennant, A. F., 1991. *The QDP/PLT User's Guide*, NASA.

Ulrich, M.-H., 1989. In: *BL Lac Objects*, eds Maraschi, L., Maccacaro, T. & Ulrich, M.-H., Springer Verlag, Berlin.

Véron-Cetty, M.-P. & Woltjer, L. J., 1990. *Astr. Astrophys.*, **236**, 69.

Weedman, D. W., 1986. *Quasar Astronomy*, Cambridge University Press, Cambridge.

Wolter, A., Gioia, I. M., Maccacaro, T., Morris, S. L. & Stocke, J. T., 1991. *Astrophys. J.*, **369**, 314.

Woltjer, L. & Setti, G., 1982. In: *Astrophysical Cosmology*, eds Brück *et al.*, Point. Acad. Sci. Scripta Varia.